Journal of Physics: Conference Series **1596** (2020) 012062 doi:10.1088/1742-6596/1596/1/012062

Numerical implementation of a hybrid PIC-fluid framework in laser-envelope approximation

Davide Terzani[1], Pasquale Londrillo[2], Paolo Tomassini[1] and Leonida A Gizzi[1]

[1] Istituto Nazionale di Ottica, CNR, Pisa, Italy
[2] INAF Sezione di Bologna, Bologna, Italy

E-mail: `davide.terzani@ino.it`

Abstract. Particle-In-Cell (PIC) simulation are fundamental to address a detailed study of a Laser Wake Field Acceleration process. Given the ongoing development of cm−scale plasma accelerators, reduced physical models are necessary to face otherwise unfeasible predictive *start-to-end* simulations. In this context, the equation of a plasma in the cold fluid approximation can be a powerful numerical tool because the system dynamics relies on the inversion of the Euler equation on a grid, much cheaper than the usual field coupling with macroparticle motion that characterizes the standard PIC loop. We show here the implementation of a hybrid PIC-fluid framework in `ALaDyn` code that allows the bulk plasma dynamics to be quickly solved while retaining the kinetic properties by placing macroparticles on top of the fluid background.

1. Introduction

In the last decades, PIC simulations have established themselves as a powerful tool in solving the Vlasov equation, *i.e.* the plasma dynamics coupled with a self-consistent electromagnetic field. However, in most of the cases, the computational time needed to evolve the detailed system dynamics greatly exceeds the availability of resources, even when running massively parallelized codes on modern supercomputers. In fact, a strict requirement of the PIC scheme is the resolution of the smallest spatiotemporal scale present in the system even though such detail may be of no interest regarding the simulation outcomes. In Laser Wake Field Acceleration (LWFA) for example, usually the smallest scale is given by the laser wavelength ($\lambda \sim \mu$m) while the accelerated bunch has to be transported along a cm−scale plasma which translates in tens of millions *CPU hours* per run. Reduced computational models become therefore crucial to allow fast and efficient *start-to-end* simulations. In particular, both the envelope approximation [1–4] and a plasma fluid description can greatly reduce the needed computational time yet relying on a solid physical modelling.

In Sec.2, we review the newly implemented explicit solver for the laser evolution in the envelope approximation. We show that laser dynamics can be evolved in an averaged (coarse resolution) framework with a one step procedure bound by the same *CFL* condition of a standard *Yee* scheme. Such evolution can be coupled to the particle motion in the same averaged framework. In Sec.3 a solver for the plasma equation in the cold fluid approximation based on a second order *Adams-Bashfort* temporal evolution and a second order *Weighted Essentially Non-Oscillatory* spatial derivative is presented. Finally, in Sec.4, it is shown that the two

schemes can be merged, defining an hybrid framework that can boost by orders of magnitude the speed of computation.

2. Envelope approximation

In LWFA, when laser envelope scale length is well separated from its characteristic wavelength, it is convenient to describe the laser-plasma interaction in an averaged framework, where only the longest (slowest) spatial (temporal) scales are retained, in what has been called *envelope approximation* [1–4]. In fact, to assure the highest accelerating gradients, in a typical laser-plasma accelerator the ponderomotive force induced by the laser envelope must be resonant with the background plasma oscillation. By converse, the short laser wavelength does not couple efficiently with the collective plasma modes and so particle quiver motion is quickly damped after the laser passage. Plasma response to the electromagnetic forcing can be so decomposed in fast oscillations, on the laser frequency scale ω_0, about a slow secular motion on the plasma wave and laser envelope time scale ω which usually satisfies $\omega/\omega_0 = \mathcal{O}(\varepsilon)$, where $\varepsilon \ll 1$ is a small parameter.

For the sake of brevity, we do not report the derivation of the model equations, which has been treated either in a Lagrangian [1, 4] or in a Eulerian [3, 5, 6] framework. As a result, the evolution of the slow laser envelope interacting with an electron plasma is governed by the hyperbolic equation

$$\left[\partial_{t,t} - 2i\omega_0(\partial_t + c\partial_z) - c^2\nabla^2\right]\widehat{a}(\mathbf{x},t) = -\omega_p^2\chi(\mathbf{x},t,|\widehat{a}|)\widehat{a}(\mathbf{x},t), \tag{1}$$

where $\widehat{a}$ is the envelope of the vector potential normalized to $A_0 = mc^2/e$ and $\chi(\mathbf{x},t,|\widehat{a}|) = \overline{n}/\overline{\gamma}$, where the density $\overline{n}$ and the ponderomotive Lorentz factor $\overline{\gamma}$ depend only on slow coordinates, *i.e.* the $\overline{f}$ operator represents an average of f over the fast oscillations. Here, the density $\overline{n}$ is normalized to the unperturbed plasma density n_0 and ω_p represents the background plasma frequency. In the cycle-averaged framework, equations of motion for an electron take the Lagrangian form

$$\begin{aligned}
&\frac{1}{c}\frac{\mathrm{d}\mathbf{p}_\alpha(t)}{\mathrm{d}t} = -\left[\mathbf{E}(\mathbf{x}_\alpha,t) + \frac{\mathbf{v}_\alpha}{c}\times\mathbf{B}(\mathbf{x}_\alpha,t)\right] + \mathbf{F}_P(\mathbf{x}_\alpha,t),\\
&\mathbf{F}_P = -\frac{1}{2\gamma_\alpha}\frac{\nabla|\widehat{a}|^2}{2}, \quad \gamma_\alpha^2 = 1 + |\mathbf{p}_\alpha|^2 + \frac{|\widehat{a}|^2}{2},\\
&\frac{1}{c}\frac{\mathrm{d}\mathbf{x}_\alpha(t)}{\mathrm{d}t} = \mathbf{v}_\alpha = \frac{\mathbf{p}_\alpha}{\gamma_\alpha},
\end{aligned} \tag{2}$$

in which momenta are normalized to mc and particles are connected to the electromagnetic field via the standard b-spline formalism. The evolution of $\mathbf{E}(\mathbf{x},t)$ and $\mathbf{B}(\mathbf{x},t)$ (here expressed in units of a wavenumber) is governed by Maxwell's equations.

The laser-plasma coupled dynamics evolution in the envelope approximation have been implemented in several works so far [2, 4, 7–12], but the usual quoted envelope evolution operator is expressed in the reference frame comoving with the laser pulse (CRF), $\xi = z - ct$, $\tau = t$ and its inversion is performed either recurring to implicit techniques or neglecting the second order derivative $\partial_{\tau,\tau}\widehat{a}$. We found that there is no general advantage in formulating the problem in the CRF since (i) a semi-implicit solver is usually less efficient and more difficult to implement than an explicit one, (ii) a new advection term is introduced in Maxwell's equations since they are not invariant under galilean transformations, (iii) numerical dispersion can be strongly mitigated by resorting to FDTD optimized derivatives [13–16]. Following such considerations, a new fast and efficient one-step explicit solver for the laser envelope equation in the laboratory reference frame coupled with the plasma dynamics and the self-consistent electromagnetic fields

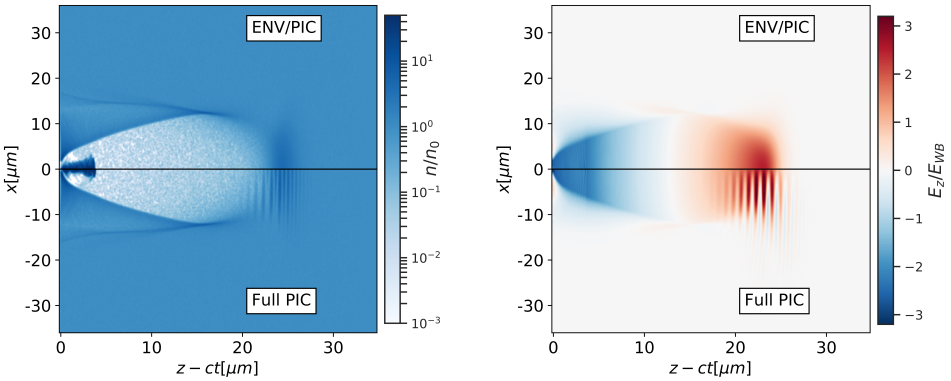

Figure 1: Comparison between full PIC and envelope simulation (ENV/PIC) performed with `ALaDyn` code. On the left, plasma densities are compared and it is clear that the injection process is correctly represented. On the right, longitudinal electric fields are shown.

has been presented and validated in [17], then also adopted in [18]. In Fig.1, we report an example of a laser propagation inside a plasma computed using both the full PIC and the PIC in envelope approximation (ENV/PIC). The laser pulse propagates for 500µm in an initially uniform plasma. Its wavelength is $\lambda_0 = 0.8$µm, $a_0 = 5$, duration $\tau_{fwhm} = 12$fs and waist $w_0 = 10$µm. The unperturbed plasma density is $n_0 = 4.3 \times 10^{18}\text{cm}^{-3}$ and the cell size in both cases is $\Delta z = \lambda_0/24$, $\Delta x = \Delta y = 4\Delta z$. Both the envelope and the electromagnetic solvers are equipped with optimized longitudinal derivatives, in order to strongly reduce the numerical dispersion effects as described in [17].

To the best of our knowledge, no reflecting or absorbing boundary condition has ever been introduced for the envelope equation. In `ALaDyn`, after an empirical validation, we found a stable boundary condition via a second order interpolation of the laser envelope on the ghost points outside the box. Anyway, we do not consider such choice as definitive and we envisage investigating this aspect in the future.

3. Plasma evolution in fluid approximation

When specific plasma kinetic effects, like self-injection and bunch acceleration are not considered, the plasma wave system away from particle crossing (wave-breaking) pathology, can be adequately described by Euler equations in collisionless cold approximation. In this framework, the Lagrangian system of equations (2) averaged over the particle distribution function in velocity space allows a reformulation of the dynamics in term of a fluid density $n(\mathbf{x}, t)$ and momentum density $\mathbf{p}(\mathbf{x}, t)$, given by

$$\begin{aligned} &\partial_t n + \nabla(n\mathbf{v}) = 0, \quad \partial_t \mathbf{p} + (\mathbf{v}\cdot\nabla)\,\mathbf{p} = \mathbf{F}_{tot}, \\ &\mathbf{F}_{tot} = -\left[\mathbf{E}(\mathbf{x},t) + \frac{\mathbf{v}}{c}\times\mathbf{B}(\mathbf{x},t)\right] + \mathbf{F}_P(\mathbf{x},t), \end{aligned} \tag{3}$$

still retaining the separation between the Lorentz force induced by the slow electromagnetic field (wakefield) and the ponderomotive force associated to the laser pulse. A simplified Euler-Maxwell description is a powerful tool both from a theoretical and a numerical point of view, in particular when performing long term integration of plasma dynamics, *e.g.* in start-to-end simulations of a LWFA, when even the envelope approximation does not sufficiently reduce the total computational time.

Implementation of a Euler-Maxwell solver presents several nontrivial problems related to numerical instabilities that can be triggered even by a moderately steep solution [19, 20]. For

nonlinear systems of fluid equations, several techniques have been proposed to capture and propagate discontinuous solutions, but they most of all refer to hyperbolic equations expressed in conservative form. A scheme based on the combination of a second order *Adams-Bashfort* (AB) temporal integrator coupled with a second order *Weighted Essentially Non-Oscillatory* (WENO) upwind derivative has been proposed to obtain a stable and robust numerical scheme that takes into account the non-conservative structure of Eq.(3) [17].

One step AB integrator for the system of equations (3), allows a consistent coupling with the FDTD scheme for the evolution of the wakefield electromagnetic field. In this framework, given the evolution equation (3) in the form $\partial_t u(\mathbf{x},t) = S[u,\mathbf{x},t]$, for $u = [\mathbf{p},n]^T$ and $S = \left[-(\mathbf{v}\cdot\nabla)\,\mathbf{p} + \mathbf{F}_{tot}, -\nabla(n\mathbf{v})\right]^T$, the discrete temporal advancement of u in the time interval $[t^n,\, t^{n+1}]$ can be written as

$$u^{n+1} = u^n + \frac{\Delta t}{2}\left[3S^n - S^{n-1}\right], \tag{4}$$

where only source terms at the current and previous integer times are involved.

The fluid density and momentum are spatially discretized on the integer nodes of the Yee grid having a cell size $\Delta\mathbf{x}_g = (\Delta x, \Delta y, \Delta z)$, *i.e.* any point $\mathbf{x}_g = (x_i, y_j, z_k)$ is identified by the triple $(i,j,k) \in \mathbb{Z}^3$. The WENO reconstruction technique presents several advantages with respect to a standard fixed-stencil upwind (or central) derivative in computing the source term on the grid points, that is $S\left[u(\mathbf{x}_g), \mathbf{x}_g, t\right]$. In fact, (i) it assures an high order (it depends on the order of the chosen scheme) accuracy on the reconstructed derivative for smooth solutions, (ii) for steep gradients, it reduces to a second order upwind scheme, preventing the numerical instability growth [21, 22], (iii) it can be conveniently extended to the case of a non-conservative system. For the detailed definition of the interpolating functions and *smoothness* coefficients in a finite difference WENO implemetation, we refer to [21, 23]. Choosing the second order accuracy scheme, the pointwise source term can be approximated as

$$S\left[u(\mathbf{x}_g), \mathbf{x}_g, t\right] \simeq S[u,\mathbf{x},t] + \mathcal{O}\left(\Delta\mathbf{x}_g^3\right). \tag{5}$$

At last, outflow boundary conditions are implemented using second order upwind scheme on a fixed stencil.

An intensive numerical benchmark of the Euler-Maxwell solver here presented has been carried out in [17]; in particular Figs.8 and 10 of [17] present a comparison of an ENV/PIC and a fluid simulation (here and from now on denoted with ENV/Fluid). We point out that a grid based code does not suffer in principle for the load unbalance that characterizes a macroparticle based code. For this reason, the execution speed does not decrease during evolution despite `ALaDyn` not having a load balancing procedure implemented. Moreover we estimate a computational cost of the order of a same resolution PIC code using second order shape functions with a single macroparticle per cell.

4. Hybrid particle-fluid dynamics

The numerical framework described in Sec.3 to construct the solution of the cold collisionless Euler equation, is suitable to be combined with a standard PIC representation, allowing the dynamical description of an electromagnetic field coupled with both a plasma bulk expressed in the cold fluid approximation and Lagrangian particles moving on top of that. At the present time, many LWFA injection and acceleration schemes are in fact intensively investigated to work in nonlinear regimes far from the wavebreaking and the self-injection threshold. It has been seen that despite the highest accelerating gradients achievable, bunches produced in these regimes may retain poor quality and may be difficult to control due to the high energy spread and slice energy spread induced by the accelerating field [24, 25]. To evolve a particle bunch injected

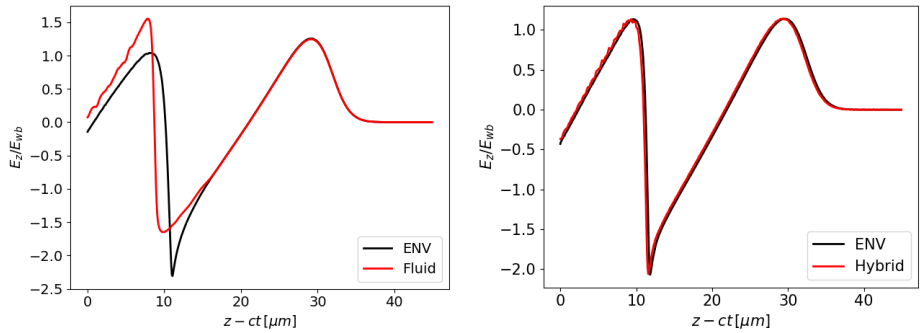

Figure 2: Comparison between longitudinal accelerating fields produced by the ENV/PIC and the ENV/Fluid schemes. A laser pulse having $a_0 = 2.4$, $w_0 = 28\mu$m, $\tau_{fwhm} = 30$fs is travelling in a uniform plasma of density $n_0 = 4 \times 10^{18}\text{cm}^{-3}$. On the left, the fluid approximation alone is not suitable to evolve plasmas that have crossed the wavebreaking limit. On the right, placing one macroparticle per cell allows to recover the expected behaviour.

in a plasma whose behaviour is well described by Eq.(3), kinetic effects (*i.e.* macroparticles) are only needed for the bunch itself, and one could strongly decrease the total computational time by substituting the background plasma macroparticles with the AB-WENO solver. Also, an *hybrid* (Eulerian and Lagrangian) numerical scheme is able to grasp the feature of a system close to the wavebreaking regime as it can be seen in Fig.2. As a matter of fact, fluid equations cannot describe the trajectory crossing of plasma particles and they tend to regularize the solution of the equations of motion, which therefore diverge from the expected one after the discontinuity ($z - ct \simeq 10\mu$m). On the other hand, the correct behaviour is recovered inserting one macroparticle per cell. We want to stress that such a poor number of macroparticles would not have been enough to perform a reliable simulation without introducing a dominant numerical noise [26]. Instead, the fluid background compensates for this lack, reinstating a dynamics that does not present statistical fluctuations, with whom the macroparticles interact.

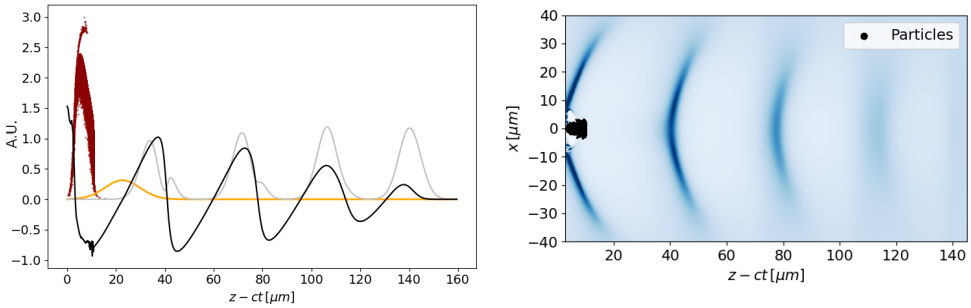

Figure 3: Production of ionized and trapped particles in the ReMPI scheme, simulated using the ENV/Fluid scheme in `ALaDyn`. On the left, the accelerating field (black), the train of pulse (grey), the ionizing pulse (yellow) and the longitudinal particle phase space (red) are represented. Quantities have been represented in arbitrary units in order to be overlapped and compared on the same plot. On the right, the resulting density map is shown, where every black dot represent a numerical particle. As it can be seen, they are only forming the accelerating bunch, whereas the background plasma density is fluid.

When computing the total current in an hybrid scheme, one has to weight the contribution of the fluid and macroparticle density respectively. The choice is not unique, and can influence both the outcome of the simulation and the numerical performance. If $\alpha \gtrsim 0$, where $\alpha = w_{MP}/(w_{MP} + w_F)$ is the relative weight of the macroparticles in the total (*i.e.* fluid plus macroparticles) density, we can expect an overall behaviour very close to a purely fluid dynamics. In addition to this, we can employ only few macroparticles since the statistical noise will not be dominant. On the other hand, when $\alpha \lesssim 1$, the fluid contribution is weak and more macroparticles are needed in order to achieve reliable results. Becomes clear that optimization of the α parameter strongly depends on the physics involved and, at the present time, we cannot recommend any specific recipe to do so.

The composite AB-WENO plus envelope solver has been implemented in the code `ALaDyn` [17, 27, 28] and has been used in the numerical validation of the Resonant Multi-Pulse Ionization injection scheme (ReMPI) proposed within the EuPRAXIA project as an ultra high quality injection and acceleration scheme [29–31]. A train of four laser pulses travels in a mixture of Helium and Nitrogen exciting a wakefield via a resonant process while staying below both the wavebreaking and the ionization injection threshold. A subsequent frequency tripled pulse ionizes the 5th atomic level of Nitrogen and the produced particles are injected and accelerated in the wakefield, resulting in an electron beam of outstanding quality. Such complex setup would not have been feasible with a reasonable computational cost with a standard PIC. Instead, the ENV/Fluid scheme allowed for fast simulations since the plasma bulk was evolved according to the fluid equations and the macroparticles only represented the few ionized and trapped particles forming the electron bunch. Background Nitrogen atoms are kept in the simulation as immobile particles, *i.e.* they do not participate as a computational load during particle motion, therefore they can be ionized employing the well-established *ADK* model. Extracted macroparticles interact with the electromagnetic field and may be trapped in the wakefield.

5. Conclusions

We have reviewed an explicit solver for the laser envelope dynamics first presented in [17] and we have introduced a new implementation of an hybrid framework, in which macroparticles' dynamics is coupled with a plasma bulk considered in a cold fluid approximation. The fast fluid solver (having a speed about the same resolution PIC code with 1 macroparticle per cell), which correctly describes plasma dynamics below the wavebreaking threshold, interacts with a few macroparticles that take into account any kinetic property of the system without considerably loading the computation. We made use of the implemented schemes to validate numerically a novel and promising injection scheme that required predictive simulation that could not be addressed with a standard PIC code. As a matter of fact, the envelope description, which does not resolve the laser wavelength, and the hybrid framework, enabled us to perform an intensive parametric scan of the system.

We point out that the fluid and hybrid `ALaDyn` features are still under an intensive investigation since the stability of the employed schemes presents some issues when the dynamics is close to the wavebreaking regime. More work to improve this aspect is expected in the near future. We acknowledge the S. Sinigardi grant IsB18_ALaRe at CINECA under the ISCRA initiative for the HPC resources.

References

[1] Startsev E and McKinstrie C 1997 *Physical Review E* **55** 7527

[2] Gordon D, Mori W and Antonsen T 1999 *APS Division of Plasma Physics Meeting Abstracts*

[3] Mora P and Antonsen Jr T M 1997 *Physics of Plasmas* **4** 217–229

[4] Cowan B, Bruhwiler D, Cormier-Michel E, Esarey E, Geddes C, Messmer P and Paul K 2011 *Journal of Computational Physics* **230** 61–86

[5] Mora P and Antonsen Jr T M 1996 *Physical Review E* **53** R2068

[6] Quesnel B and Mora P 1998 *Physical Review E* **58** 3719

[7] Gordon D F 2007 *IEEE transactions on plasma science* **35** 1486–1488

[8] Benedetti C, Schroeder C, Esarey E, Geddes C and Leemans W 2010 *AIP Conference Proceedings* vol 1299 (AIP) pp 250–255

[9] Tomassini P and Rossi A 2015 *Plasma Physics and Controlled Fusion* **58** 034001

[10] Benedetti C, Rossi F, Schroeder C, Esarey E and Leemans W 2015 *Physical Review E* **92** 023109

[11] Helm A, Vieria J, Silva L and Fonseca R 2016 *APS Division of Plasma Physics Meeting 2016, abstract id. GP10.011*

[12] Benedetti C, Schroeder C, Geddes C, Esarey E and Leemans W 2017 *Plasma Physics and Controlled Fusion* **60** 014002

[13] Karkkainen M, Gjonaj E, Lau T and Weiland T 2006 *Proceedings of ICAP* vol 1 p 35

[14] Londrillo P, Benedetti C, Sgattoni A and Turchetti G 2010 *Nuclear Instruments and Methods in Physics Research, Sec. A* **620**(1) 28–35

[15] Pukhov A 2015 *arXiv preprint arXiv:1510.01071*

[16] Lehe R, Lifschitz A, Thaury C, Malka V and Davoine X 2013 *Physical Review Special Topics-Accelerators and Beams* **16** 021301

[17] Terzani D and Londrillo P 2019 *Computer Physics Communications* **242** 49–59

[18] Massimo F, Beck A, Dérouillat J, Grech M, Lobet M, Pérez F, Zemzemi I and Specka A 2019 *Plasma Physics and Controlled Fusion* **61** 124001

[19] LeVeque R J 1990 *Conservative methods for nonlinear problems* (Springer) pp 122–135

[20] LeVeque R J 2002 *Finite volume methods for hyperbolic problems* vol 31 (Cambridge university press)

[21] Xu-Dong Liu S O and Chang T 1994 *Journal of Computational Physics* **115** 200–212

[22] Balsara D S 2017 *Living reviews in computational astrophysics* **3** 2

[23] Shu C W and Osher S 1988

[24] Aßmann R and Grebenyuk J 2014

[25] Li X, Nghiem P A P and Mosnier A 2018 *Physical Review Accelerators and Beams* **21** 111301

[26] Birdsall C K and Langdon A B 2004 *Plasma physics via computer simulation* (CRC press)

[27] Benedetti C, Sgattoni A, Turchetti G and Londrillo P 2008 *IEEE Transactions on plasma science* **36** 1790–1798

[28] Terzani D, Sinigardi S, Londrillo P, Marocchino A, Massimo F, Mira F and Sgattoni A 2020 Aladyn/aladyn: Aladyn v2020.2 URL `https://doi.org/10.5281/zenodo.3630598`

[29] Tomassini P, De Nicola S, Labate L, Londrillo P, Fedele R, Terzani D and Gizzi L A 2017 *Physics of Plasmas* **24** 103120

[30] Tomassini P, Terzani D, Labate L, Toci G, Chance A, Nghiem P A P and Gizzi L A 2019 *Physical Review Accelerators and Beams* **22** 111302

[31] Nghiem P A P, Alesini D, Aschikhin A, Assmann R, Audet T, Beck A, Chancé A, Chen M, Chiadroni E, Cianchi A *et al.* 2019 *Journal of Physics: Conference Series* vol 1350 (IOP Publishing) p 012068